, ,

Discrete Ordinates and Monte Carlo Methods for Radiative Transfer Simulation applied to CFD combustion modelling

David Joseph and Patrice Perez

Centre de Recherche d'Albi en génie des Procédés des Solides Divisés, de l'Energie et de l'Environnement, 81000 Albi, France and HPC-SA 3, Chemin du Pigeonnier de la Cépière, Toulouse, France

Mouna El Hafi*

Centre de Recherche d'Albi en génie des Procédés des Solides Divisés, de l'Energie et de l'Environnement, 81000 Albi, France

Bénédicte Cuenot

C.E.R.F.A.C.S. 42, Av. Gaspard Coriolis, Toulouse, France

(Dated: February 29, 2008)

Abstract

Modelling radiative heat transfer in combustion applications involving complex geometries and detailed spectral properties of radiative gaseous species remains a difficult challenge, especially when full coupling with detailed chemistry and fluid dynamics is required. The Monte Carlo Method (MCM) usually considered as a reference "exact" method for the computation of radiative transfer is however very demanding in CPU-time. An alternative is the Discrete Ordinates Method (DOM), based on a finite volume approach, that is more suitable for a direct coupling with CFD but may lack accuracy. The aim of the present paper is to propose and demonstrate the efficiency of a methodology for radiative transfer calculation, combining the advantages of both MCM and DOM. In this approach, the fast DOM is used to compute the radiative solution, whose accuracy is then controlled by comparison with the "exact" MCM solution at a selection of controlling points. A first application of the proposed methodology to an industrial burner prototype shows its validity and potential for the direct coupling of radiation calculations with reacting flow computations.

Keywords: Radiative heat transfer, Unsteady combustion, Monte Carlo, Discrete Ordinates, Three-dimensional geometries

Combustion simulation involves the treatment of coupled phenomena such as detailed chemistry, fluid mechanics and heat transfer for three-dimensional systems in complex geometries. The accurate treatment of thermal radiation is crucial if the aim is to predict the concentration of minor species, soot or wall heat fluxes that are highly dependent on temperature levels. However the detailed calculation of radiative transfer leads to prohibitive computing time. This is even more critical for unsteady combustion simulations, where the full coupling with radiation is required.

The optically thin assumption is commonly used for the calculation of radiation in combustion simulations. In this approximation, the absorption of the gas mixture is neglected and only the emitted part of the radiative flux is considered, which considerably simplifies the calculation. If this assumption is valid for small scale flames with thin opacities, it is not anymore the case for large scale furnaces or luminous flames. For instance, in fire pool applications, radiation is one of the most important heat transfer phenomena. In smaller industrial burners, it is known that the NO_x emission and soot production are very sensitive to radiation [1, 2]. Wall heat fluxes are also critical parameters in burner design and should include radiative heat transfer [3].

In a recent work, Jensen et al. [4] compare the usual numerical methods for solving the Radiative Transfer Equation (RTE). The Ray Tracing and Monte Carlo Methods (MCM) [5–8] allow to calculate quasi-exact solutions and are considered as reference methods. In addition, MCM also provides estimates of the errors associated to the solution. It is able to treat high levels of complexity (complex geometries, reflective walls, scattering medium, gas spectral properties, ..) and there is no conceptual difficulties to realize the coupling with flow dynamics. However these methods are complex and result in very high CPU costs. Many interesting ideas are actually under progress to reduce the computation time. Among them, the sensitivity approach (using first order of Taylor expansion) has been already tested in several applications [9, 10] and showed a good potential. Despite these improvements, the direct coupling of MCM with flow simulations is still not possible. On the contrary, the Moment method [11], Discrete Ordinates Method (DOM) [12, 13] and the Discrete Transfer Method [14] are fast and easy to couple with fluid dynamics, but they give approximate solutions. In particular the DOM is highly sensitive to the angular

(Ray effect) and spatial discretization. In [4], it is shown however that the DOM using the S_4 quadrature (24 discrete directions) already offers a very good compromize between CPU-time and accuracy, and that the use of a higher order quadrature, such as the LC_{11} quadrature (96 discrete directions), provides accuracy levels comparable to the quasi-exact methods (MCM and Ray Tracing).

It is possible to take advantage of the availability of the two classes of methods by combining them in a global methodology, allowing fast radiation calculations with a systematic estimation and control of the error. The simultaneous use of the pair DOM/MCM is then an optimal compromise between CPU cost and accuracy in view of coupled combustion-radiation simulations. The benefit of this approach is double : first, it allows to validate the DOM solution, and second it determines the level of accuracy of the various approximations in order to optimize the set of parameters (number of directions, discretization scheme, ..). The objective of the present paper is to describe the proposed appoach and demonstrate its validity and potential for coupled radiation-combustion simulations on different test cases.

Compared to most existing radiation codes, the coupling of radiation with combustion requires additional developments. First, the complexity of real industrial geometries require the use of unstructured grids. For an efficient coupling, the radiative transfer model should be able to work on the same mesh than the combustion simulation and therefore handle unstructured meshes. Second, the description of the gaseous radiative properties has to be in accordance with the combustion simulations accuracy. In this context, two radiative transfer codes, DOMASIUM (based on DOM) and MCRAD (based on MCM), have been developed and applied to an unsteady combustion application following the above methodology.

In the first section, the DOM and the MCM are briefly described. In the second section, the DOM code, specifically developed for unstructured meshes, is validated against MCM on a non-isothermal and non-homogeneous test case in a cylindrical geometry. The last section is devoted to the computation of thermal radiation in a real combustion chamber involving a complex geometry with an unstructured grid, using the combination of both DOM and MCM as explained above.

MATHEMATICAL FORMULATION

The two radiation codes DOMASIUM and MCRAD used in the present study were initially developed by D. Joseph [15] and P. Perez [16]. DOMASIUM is detailed in [13]. MCRAD has been utilized for benchmark publications and is described in [6, 7]. The two codes have also been used in a pool fire problem where they have been compared to a Ray Tracing method, a Discrete Transfer Method and a Moment Method [4], showing a good agreement with the reference solutions.
In all calculations presented in this paper, the same gas radiation property model (the Statistical Narrow-Band Correlated-K model [17, 18]) has been used. It is also described below.

Discrete Ordinates Method (DOM)

DOMASIUM [4, 13] has been designed to simulate the radiative heat transfer in coupled simulations with flow dynamics, involving unstructured grids. In the following and for sake of clarity, the intensities and radiative properties are expressed for a single wavenumber (monochromatic case) but the formulation can be easily extended to a full spectrum.
Discrete Ordinates Method have been introduced first by [19] and have been widely used in radiative transfer applications. Considering an absorbing-emitting and non-scattering gray medium, the variation of the radiative intensity $I(\mathbf{s})$ along a line of sight can be written as:

$$\frac{dI(\mathbf{s})}{ds} = \kappa I_b - \kappa I(\mathbf{s}) \tag{1}$$

where $I(\mathbf{s})$ is the radiative intensity along the directional coordinate $\mathbf{s}$, I_b is the blackbody radiative intensity, and κ is the absorption coefficient. Boundary conditions for diffuse surfaces are taken from the relation giving the intensity leaving the wall I_w as a function of the blackbody intensity of the wall $I_{b,w}$ and of the incident radiative intensity:

$$I_w(\mathbf{s}) = \epsilon_w I_{b,w} + \frac{\rho_w}{\pi} \int_{\mathbf{n}.\mathbf{s'}<0} I_w(\mathbf{s'}) |\mathbf{n}.\mathbf{s'}| d\Omega' \tag{2}$$

where ϵ_w is the wall emissivity, ρ_w the wall reflectivity, $\mathbf{n}$ the unit vector normal to the wall and $\mathbf{s'}$ the direction of propagation of the incident radiation confined within a solid angle $d\Omega'$.

Angular discretization

In the DOM, the calculation of a radiative source term at a given point is based on the discretization of the Radiative Transfer Equation (Eq.1) according to a chosen number N_{dir} of discrete directions $\mathbf{s}_i(\mu_i, \eta_i, \xi_i)$, associated to the corresponding weights w_i, contained in the solid angle 4π, and where (μ_i, η_i, ξ_i) are directional cosines. Different angular discretizations may be used. In a recent study, Koch and Becker [20] compare the efficiency of several types of angular quadratures. They recommend the LC_{11} quadrature for its better accuracy. However calculations performed with the S_4 quadrature satisfy a good compromise between accuracy and rapidity as shown in [4], and may also be used.

Spatial discretization for hybrid grids

The RTE (Eq.1) is solved for every discrete direction $\mathbf{s}_i$ using a finite volume approach. The integration of the RTE over the volume V of an element limited by a surface Σ, and the application of the divergence theorem yields:

$$\int_{\Sigma} I(\mathbf{s}_i).\mathbf{s}_i.\mathbf{n}d\Sigma = \int_{V} (\kappa I_b - \kappa I(\mathbf{s}_i))dV \tag{3}$$

The domain is discretized in three-dimensional control volumes V. It is assumed that I_b and $I(\mathbf{s}_i)$ are constant over the volume V and that the intensities I_j at the faces are constant over each face. Considering that I_j is the averaged intensity over the j^{th} face, associated with the center of the corresponding face, that $I_{b,P}$ and I_P are the averaged intensities over the volume V, associated with the center of the cell, and assuming plane faces and vertices linked by straight lines, Eq.(3) can be discretized as follows :

$$\sum_{j=1}^{N_{face}} I_j(\mathbf{s}_i).(\mathbf{s}_i.\mathbf{n}_j)A_j = \kappa V(I_{b,P} - I_P(\mathbf{s}_i)) \tag{4}$$

where $\mathbf{n}_j$ is the outer unit normal vector of the surface j.

The scalar product of the i^{th} discrete direction vector with the normal vector of the j^{th} face of the considered cell is defined by D_{ij}:

$$D_{ij} = \mathbf{s}_i.\mathbf{n}_j = \mu_i n_{xj} + \eta_i n_{yj} + \xi_i n_{zj} \tag{5}$$

The discretization of the boundary condition (Eq.(2)) is straightforward:

$$I_w = \epsilon_w I_{b,w} + \frac{1-\epsilon_w}{\pi} \sum_{\mathbf{n}.\mathbf{s}_i<0} w_i I(\mathbf{s}_i) \mid \mathbf{n}.\mathbf{s}_i \mid \tag{6}$$

For each cell, the incident radiation G is evaluated as follows:

$$G = \int_{4\pi} I(\mathbf{s}) d\Omega \simeq \sum_{i=1}^{N_{dir}} w_i I(\mathbf{s}_i) \tag{7}$$

and the incident heat flux H_w at the wall surfaces is :

$$H_w = \int_{\mathbf{n}.\mathbf{s}<0} I(\mathbf{s}) \mid \mathbf{n}.\mathbf{s} \mid d\Omega \simeq \sum_{\mathbf{n}.\mathbf{s}_i<0} w_i I_i \mid \mathbf{n}.\mathbf{s}_i \mid \tag{8}$$

For a gray medium, the radiative source term S_r is given by:

$$S_r = \nabla . Q_r = \kappa(4\pi I_b - G) \tag{9}$$

where Q_r is the radiative heat flux, and the radiative net heat flux at the wall is:

$$Q_w = \epsilon \pi I_{b,w} - H \tag{10}$$

For the evaluation of the radiative intensity $I(\mathbf{s}_i)$ in Eq. (6) to (10) Ströhle et al. [21] proposed a simple spatial differencing scheme based on the mean flux scheme that proved to be very efficient in the case of hybrid grids. This scheme relies on the following formulation:

$$I_P = \alpha \overline{I_{out}} + (1 - \alpha) \overline{I_{in}} \tag{11}$$

where $\overline{I_{in}}$ and $\overline{I_{out}}$ are respectively the intensities averaged over the entering and the exit faces of the considered cell. α is a weighting number between 0 and 1. Substituting $\overline{I_{out}}$ from Eq.(11) into Eq.(4) yields (for more details see [13]):

$$I_P = \frac{\alpha V \kappa I_b - \sum\limits_{\substack{j \\ D_{ij}<0}} D_{ij} A_j I_j}{\alpha \kappa V + \sum\limits_{\substack{j \\ D_{ij}>0}} D_{ij} A_j} \tag{12}$$

The case $\alpha = 1$ corresponds to the Step scheme used by Liu et al. [12]. The case $\alpha = 0.5$ is called Diamond Mean Flux Scheme (**DMFS**) which is formally more accurate than the Step scheme. After calculation of I_P from Eq.(12), the radiation intensities at cell faces such that $D_{ij} > 0$ are set equal to $\overline{I_{out}}$, obtained from Eq.(11). For a given discrete direction, each face of each cell is placed either upstream or downstream of the considered cell center (a face parallel to the considered discrete direction plays no role). The control volumes are treated following a sweeping order such as the radiation intensities at upstream cell faces are

known. This order depends on the discrete direction under consideration. An algorithm for the optimization of the sweeping order has been implemented [13]. Note that this sweeping order is stored for each discrete direction, and only depends on the chosen grid and the angular quadrature, i.e. it is independent on the physical parameters or the flow and may be calculated only once, prior to the full computation.

Spectral gas properties

The absorption coefficient κ of the combustion products is highly dependent on the wavenumber ν as shown by line spectra of radiative gases (H_2O, CO_2 and CO). To take into account this spectral dependency, the absorption coefficient of each species is here represented by the *SNB-ck* model [18, 22, 23]. For the gas mixture composed of different species, the same model is used, building data according to the mixing model exposed by Liu [23]. The radiative solutions are obtained by computing $N_{bands} \times N_{quad}$ independent calculations where $N_{bands} = 367$ is the number of narrow bands of spectral width $\Delta\eta = 25\, cm^{-1}$, describing the spectral properties in the range $150 - 9300\, cm^{-1}$, and $N_{quad} = 5$ is the number of the Gauss-Legendre quadrature points used for the spectral integration over each narrow band. For non-gray media, introducing spectral dependencies in Eq. (9), gives for the source term :

$$S_{r,DOM} = \sum_{i=1}^{N_{band}} \sum_{j=1}^{N_{quad}} \Delta\nu_i w_{ij} \kappa_{ij} (4\pi \overline{I}_{b,ij} - G_{ij}) \tag{13}$$

where G_{ij} is obtained from Eq.(7).
The computational efficiency of such a model is strongly linked to the number of bands N_{bands}, that has to be optimized depending on the studied case.

Monte Carlo Method - Net Exchange Formulation (MCM-NEF)

The code MCRAD [4, 6] is based on MCM and uses computer graphics algorithms. It provides the radiative source terms and the wall heat fluxes as well as their associated statistical error estimates. One of the main features of the MCM used here is the Net Exchange Formulation (NEF). This NEF presents some similarities with the zonal method proposed by Hottel [24]. This formulation that satisfies the reciprocity principle was first introduced by Green [25] in 1967. It has been applied to one-dimensional radiative heat

transfer problems [5, 26], to multidimensional problems [6, 7], and very recently, to fires for benchmark solutions [4]. The NEF is the integral formulation of the radiative heat transfer, using shape factors between two volumes (Eq. 14), a surface and a volume (Eq. 15) or two surfaces (Eq. 16) respectively :

$$\zeta_{ij,\nu}^{VV} = \int_{V_j}\int_{V_i} \frac{\kappa_i \kappa_j \tau_{\nu,ij}}{s_{ij}^2}\, dV_i dV_j \tag{14}$$

$$\zeta_{ij,\nu}^{VS} = \int_{S_j}\int_{V_i} \frac{\kappa_i . |\mathbf{n}_j . \mathbf{s}| . \tau_{\nu,ij}}{s_{ij}^2}\, dV_i dS_j \tag{15}$$

$$\zeta_{ij,\nu}^{SS} = \int_{S_j}\int_{S_i} \frac{|\mathbf{n}_i . \mathbf{s}| . |\mathbf{n}_j . \mathbf{s}| . \tau_{\nu,ij}}{s_{ij}^2}\, dS_i dS_j \tag{16}$$

with $\tau_\nu(s_{ij})$ the spectral transmissivity along a straight line between two points P_i and P_j expressed as :

$$\tau_\nu(s_{ij}) = exp\Big[- \int_{s_i}^{s_j} \kappa_\nu(s) ds \Big] \tag{17}$$

and $\Delta I_{b,\nu}$ the black intensity difference between these points :

$$\Delta I_{b,\nu} = I_{b,\nu}(P_i) - I_{b,\nu}(P_j) \tag{18}$$

These definitions allow the respective net exchange calculation :

$$\varphi_{(V_i,V_j)} = \int_0^\infty \zeta_{ij,\nu}^{VV} \Delta I_{b,\nu}\, d\nu \tag{19}$$

$$\varphi_{(V_i,S_j)} = \int_0^\infty \zeta_{ij,\nu}^{VS} \Delta I_{b,\nu}\, d\nu \tag{20}$$

$$\varphi_{(S_i,S_j)} = \int_0^\infty \zeta_{ij,\nu}^{SS} \Delta I_{b,\nu}\, d\nu \tag{21}$$

where φ represents the net radiative exchange between two volumes, a volume and a surface or two surfaces. The generalization of these terms to non black walls can be found in [7]. The radiative source term for a volume V_i or the net heat flux at a surface S_i are computed by summing their radiative exchanges with all the other volumes and surfaces :

$$\int_{V_i} S_r(\mathbf{r}_{P_i})\, dV_i = \sum_{j=1}^{N_s} \varphi_{(V_i,S_j)} + \sum_{j=1}^{N_v} \varphi_{(V_i,V_j)} \tag{22}$$

and

$$q_{w,net,i} = \frac{\sum_{j=1}^{N_s} \varphi_{(S_i,S_j)} + \sum_{j=1}^{N_v} \varphi_{(S_i,V_j)}}{S_i} \tag{23}$$

where N_s is the number of surfaces and N_v the number of volumes. The multiple integrals encountered in Eqs.(19-21) are calculated with a Monte-Carlo Method [16]. Each radiative exchange can be represented as an integral $\mathbf{I}$ of a function g on the domain D. Defining an arbitrary probability density function p and a random variable X distributed according to p, $g(X)$ is also a random variable and $\mathbf{I}$ is the expectation of $g(X)$. $\mathbf{I}$ will be estimated with N samples of $g(X)$:

$$\mathbf{I} = E[g(X)] \approx \frac{1}{N}\sum_{i=1}^{N} g(x_i) = < g(X) >_N$$

where x_i is a realization of X. This statistical approach provides the radiative source term and the wall heat flux with an error estimate. The standard deviation of the estimate is :

$$\sigma(< g(X) >_N) = \frac{1}{\sqrt{N}}\sigma(g(X)) \tag{24}$$

where $\sigma(g(X))$ is the standard deviation of $g(X)$, and is approximated as:

$$\sigma(\mathbf{I}) \approx \frac{1}{\sqrt{N}}\sqrt{[< g(X)^2 >_N - < g(X) >_N^2]} \tag{25}$$

Note that MCRAD uses a suitable pdf p that reduces significantly the CPU-time [5].

Spectral gas properties and k-distribution formulation

The spectral integrations in Eq.(19) to (21) are carried out over narrow bands, and the k-distribution method is employed within each band. According to this method, any radiative quantity A depending on κ_ν is averaged over a band of width $\Delta\nu$ as

$$\overline{A} = \frac{1}{\Delta\nu}\int_{\Delta\nu} A(\kappa_\nu)\, d\nu = \int_0^\infty f(\kappa)A(\kappa)d\kappa \tag{26}$$

where $f(\kappa)$ is the distribution function of the absorption coefficient within a spectral narrow band [27]. In the case of gas mixture, the absorption coefficient at a given wave number is computed as the sum of the absorption coefficients of all gas species. For a mixture of H_2O, CO_2 and CO, one obtains :

$$\overline{A} = \frac{1}{\Delta\nu}\int_{\delta\nu} A\big(\kappa_{\nu,H_2O} + \kappa_{\nu,CO_2} + \kappa_{\nu,CO}\big)\, d\nu \tag{27}$$

The correlated-k assumption is considered for non homogeneous media treatment in each narrow band, so that Eqs. (19), (20) and (21) become:

$$\begin{aligned}
\varphi_{(V_i,V_j)} &= \sum_{n=1}^{n_b} \Delta\nu_n \int_0^1 dg \int_{V_i} dV_i \int_{V_j} dV_j \frac{1}{l_{ij}^2} \quad \kappa(g) \\
&\times \; exp\Big[- \int_{l_i}^{l_j} \kappa(g) dl \Big] \kappa(g) \quad \Delta I_{b,\nu} \\
\varphi_{(V_i,S_j)} &= \sum_{n=1}^{n_b} \Delta\nu_n \int_0^1 dg \int_{V_i} dV_i \int_{S_j} dS_j \frac{\vec{u}.\vec{n_j}}{l_{ij}^2} \quad \kappa(g) \\
&\times \; exp\Big[- \int_{l_i}^{l_j} \kappa(g) dl \Big] \quad \Delta I_{b,\nu} \\
\varphi_{(S_i,S_j)} &= \sum_{n=1}^{n_b} \Delta\nu_n \int_0^1 dg \int_{S_i} dS_i \int_{S_j} dS_j \frac{(\vec{u}.\vec{n_i})(\vec{u}.\vec{n_j})}{l_{ij}^2} \\
&\times \; exp\Big[- \int_{l_i}^{l_j} \kappa(g) dl \Big] \quad \Delta I_{b,\nu}
\end{aligned} \tag{28}$$

where l_{ij} is the length between points i and j, $\vec{n_i}$ and $\vec{n_j}$ are normal vectors to surfaces at point i and j, and $\vec{u}$ is the directional vector between i and j.

Combined DOM-MCM methodology

In the proposed approach, the radiative solution is calculated with the DOM using either the S_4 or LC_{11} quadrature, allowing a fast and robust computation. However the obtained solution is not exact and the error associated to each point is unknown. To evaluate the accuracy of the DOM solution, the MCM is run simultaneously to calculate the exact radiation **at selected representative points** only that play the role of probes in the complete field. The analysis of the DOM results at the same points in the light of the MCM exact solution gives a good evaluation of the full radiation field.

RESULTS

Validation test case

The test case presented here has already been described in detail in [6] where the MCM used in MCRAD, a Ray Tracing method and a DOM for structured grids were compared.

Here the same test case is used to compare the DOM solution on unstructured grids, performed on DOMASIUM, with the reference MCM solution.

The configuration is a cylindrical black walled enclosure of lenght L containing a mixture of water vapor, carbon dioxide, and nitrogen at atmospheric pressure. The geometrical characteristics are : $L = 1.2$ m and the radius is $R = 0.3$ m. The wall temperature is 800K, except at $z = L$ where it is 300K. The temperature and concentration fields are described by the following analytical functions:

$$T(z,r) = 800 + 1200(1 - r/R)(z/L) \tag{29}$$

$$X_{H_2O}(z,r) = 0.05.\left[1 - 2(z/L - 0.5)^2\right].(2 - r/R) \tag{30}$$

$$X_{CO_2}(z,r) = 0.04.\left[1 - 3(z/L - 0.5)^2\right].(2.5 - r/R) \tag{31}$$

The DOM calculation is performed using the LC_{11} quadrature and about 100,000 cells for the grid (Fig. 5).

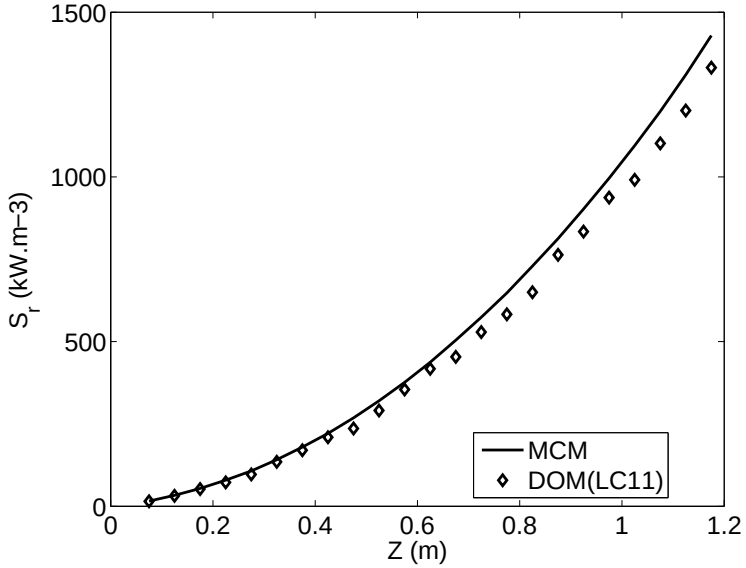

FIG. 1: Radiative source terme along the central axis of the cylinder.

The radiative source term along the central axis and the radiative heat flux at the wall are shown respectively in Fig. 1 and 3, where results from both methods DOM and MCM are plotted. The associated relative errors obtained with MCM are presented in Fig. 2 and 4. Due to the fact that the unstructured grid used for the DOM calculation does not

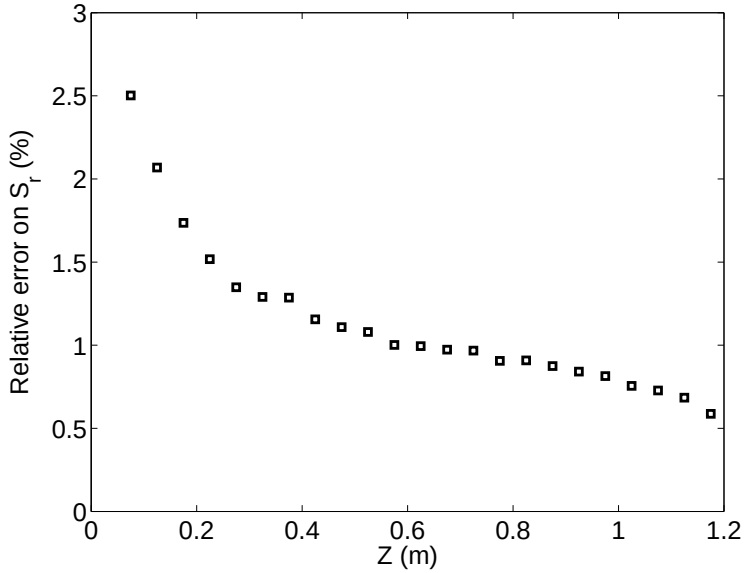

FIG. 2: Relative error associated to the MCM radiative source term along the central axis of the cylinder

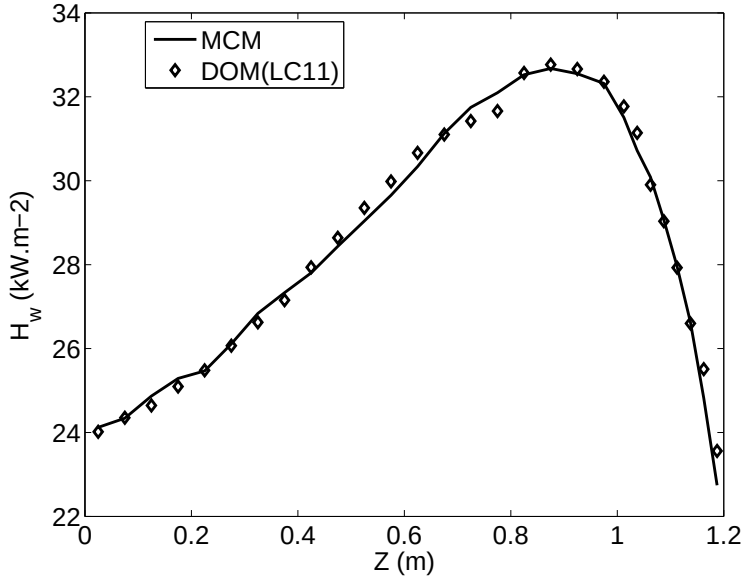

FIG. 3: Incident radiative heat flux at the wall of the cylinder.

coincide with the location of the points calulated with the MCM, an interpolation procedure is needed to allow the comparison. From the MCM error estimates, the averaged relative error is found to be about 1.13% for the radiative source term and 1.98% for the radiative

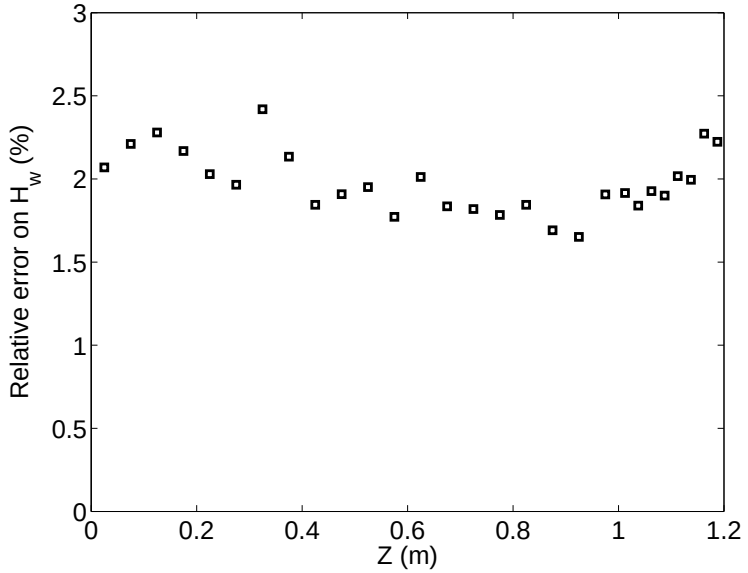

FIG. 4: Relative error associated to the MCM incident radiative heat flux at the wall of the cylinder.

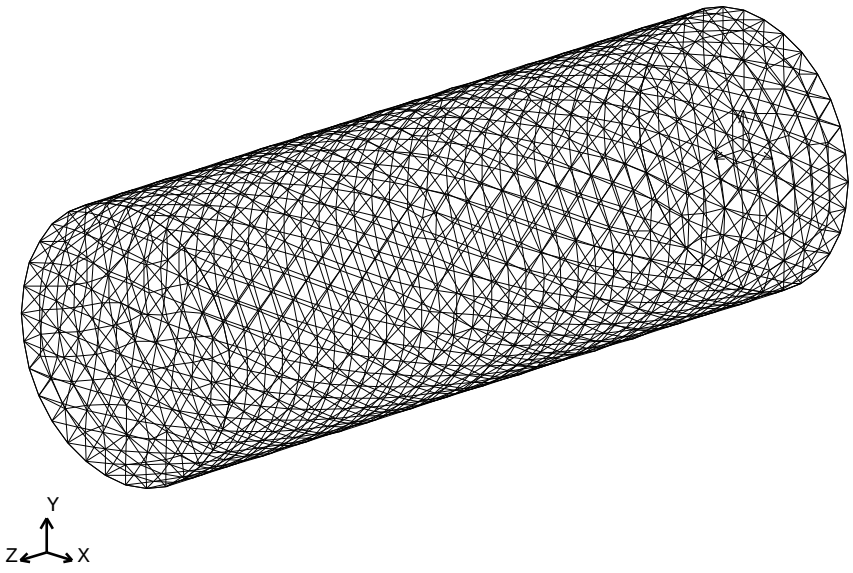

FIG. 5: Cylindrical grid (100,000 cells).

heat flux. Figure 3 demonstrates the high accuracy of the DOM for the wall heat flux. The source term (Fig. 1) calculated with DOM is also very accurate at the cold side of

the cylinder, but a small increasing discrepancy with the MCM reference solution appears in the hot half. This discrepancy however does not exceed 10 %. A first explanation may be due to the unsufficient spatial discretization, called "false scattering", as explained in the parametric study of Joseph [15]. He shows that false scattering increases in DOM for increasing optical thickness. In the present case, the temperature and concentration fields (Eqs. 29-30) lead to higher optical thicknesses on the hot side of the cylinder and false scattering is therefore likely to appear. Another reason for the difference between DOM and MCM may be attributed to the calculation of the species molar concentration and temperature fields themselves, that are discretized in the DOM but exactly computed from Eqs. 29-30 in the MCM.

Application to a real combustion chamber

The evaluation of the combined DOM-MCM methodology is now performed on a complex 3D configuration of a realistic combustion chamber (Fig. 6). Flow solutions are provided by

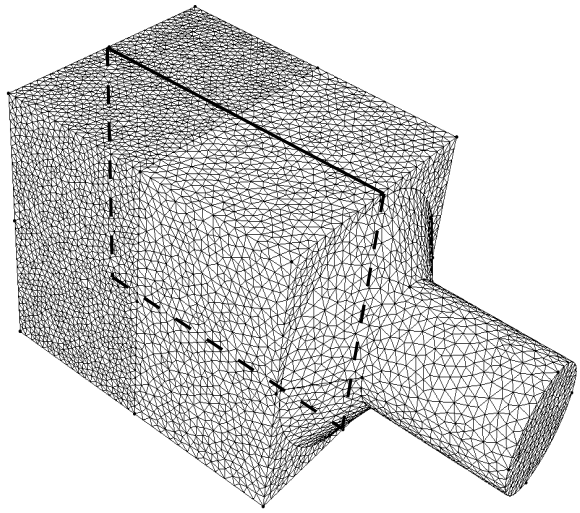

FIG. 6: Grid of the combustion chamber.

a combustion code based on the LES approach [28, 29]. In this test case, a swirled turbulent premixed flame is stabilised on a methane/air injection at a stochiometric ratio of 0.75, an

air flow rate of 12 g/s and a temperature of 300 K for a thermal power of 27 kW. The chamber has a square cross section of 86×86 mm^2 and its length is 110 mm. It ends into an exhaust duct with a 6:1 contraction. It is assumed that walls are adiabatic and may be considered as perfect radiative black bodies.

The flame/turbulence interaction is modeled by the Thickened Flame/Efficiency Function model [30, 31] and the chemical scheme for combustion takes into account two reactions with six species (CH_4, O_2, CO_2, CO, H_2O and N_2) [32]. The molar concentrations of CO_2, CO, H_2O ,O_2 and N_2 are used to determine the radiative spectral properties of the mixture. Figure 8 shows a 2D view in the cutting median plane defined on Fig. 6, of the temperature and radiative species molar fractions fields obtained from the LES and used for the radiation calculation. The corresponding heat release $\dot{\omega}$ is shown on Fig. 7. The flame has the classical

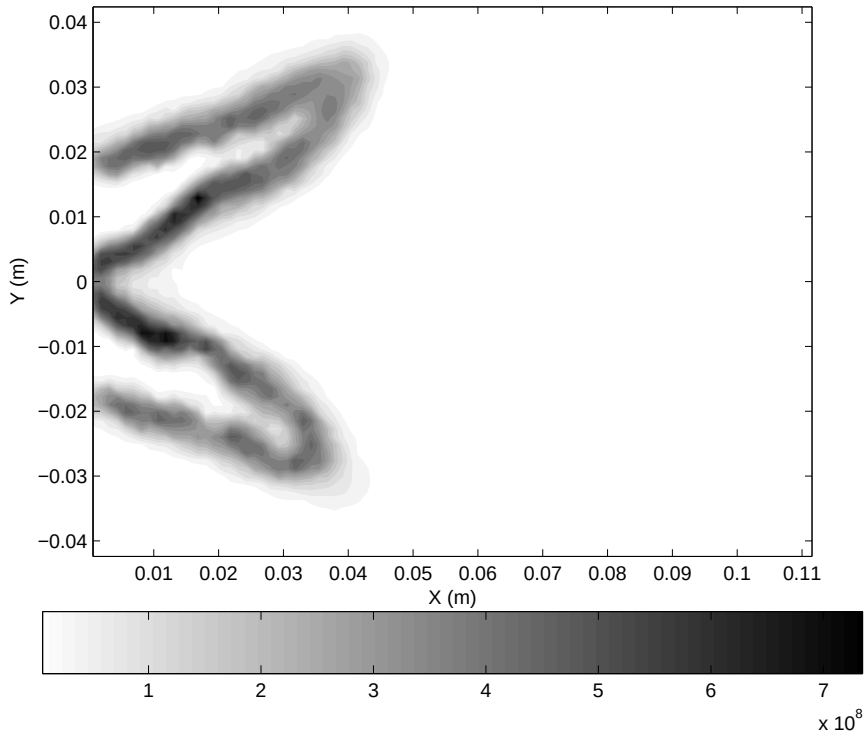

FIG. 7: Instantaneous heat release $\dot{\omega}$ in the median cutting plane of the combustion chamber.

conical shape found in this type of burners. It is attached to the injector, and deviated from the central axis by the swirling flow that creates a central recirculation zone. The maximum heat release is of the order of 7.10^8 J.m^{-3}.s^{-1}, leading to a maximum temperature of about

1900 K.

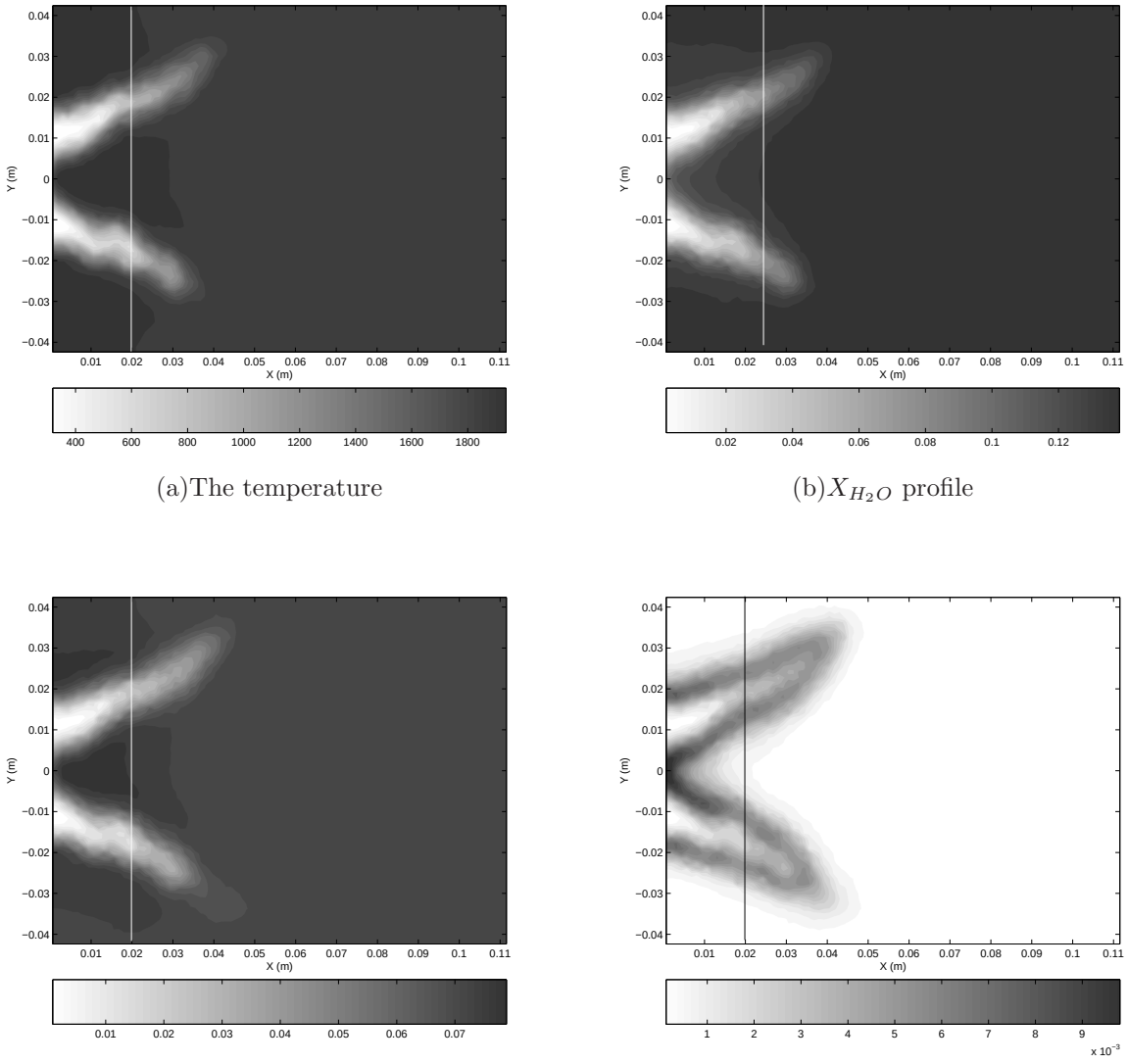

(a)The temperature

(b)X_{H_2O} profile

(c)X_{CO_2} profile

(d)X_{CO} profile

FIG. 8: Instantaneous solution fields in the median cutting plane of the combustion chamber: temperature and radiative species concentration

Figure 9 represents the corresponding instantaneous radiative source term obtained from DOM with the S_4 quadrature. The maximum value is of the order of 10^6 J.m^{-3}.s^{-1}, i.e. two orders of magnitude smaller than the maximum heat release.

However it is interesting to note that the location of the maxima of these two energy source

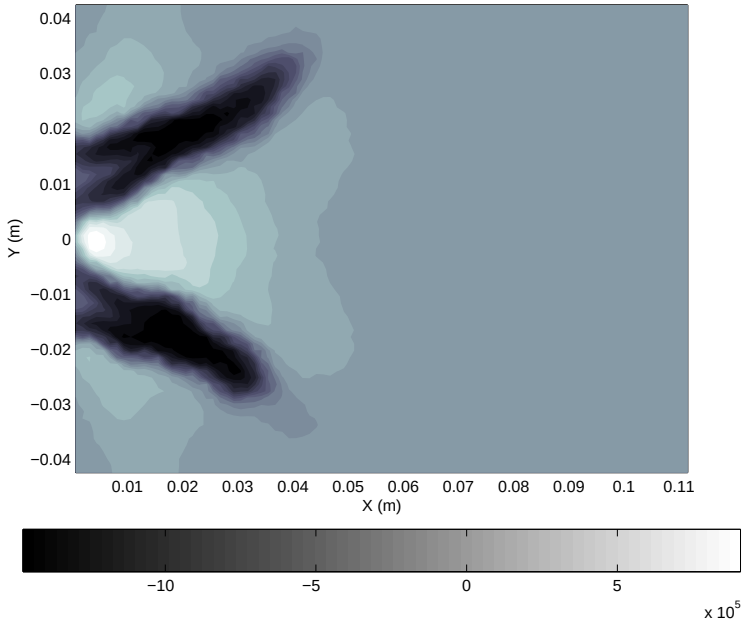

FIG. 9: Instantaneous radiative source term in the median cutting plane of the combustion chamber. Calculation with DOM-S_4 quadrature

terms is completely different: the heat release is maximum at the flame front location, i.e. at the frontier between cold and hot gas, whereas the absolute value of the radiative source term is the highest in the cold gas region, where there is strong absorption. This is due to the presence in these regions of absorbing chemical species (combustion products that have diffused in the unburnt gas) at a low temperature. This may give locally a significant contribution to the total gas energy, and finally lead to a potential high impact on the flame structure and the flow. Fig. 11 represents the emitted part E and the incident part G of the radiative heat fluxes that sum to the radiative source term S_r. It appears that the radiative exchanges E and G are of the same order of magnitude, and that both are higher than the source term. Therefore in this case, a simple model based on emission only (as the Optically Thin Model) would clearly lead to a wrong source term which is expected to have a strong impact on minor species prediction.

The same calculation was also performed with the LC_{11} quadrature and a comparison is shown on Fig. 10, where the radiative source term (Fig. 9) is plotted along a line at $x = 0.02$ m for the two DOM (S_4 and LC_{11}) and the MCM calculations. The corresponding temperature and radiative species molar fractions profiles are represented along the same

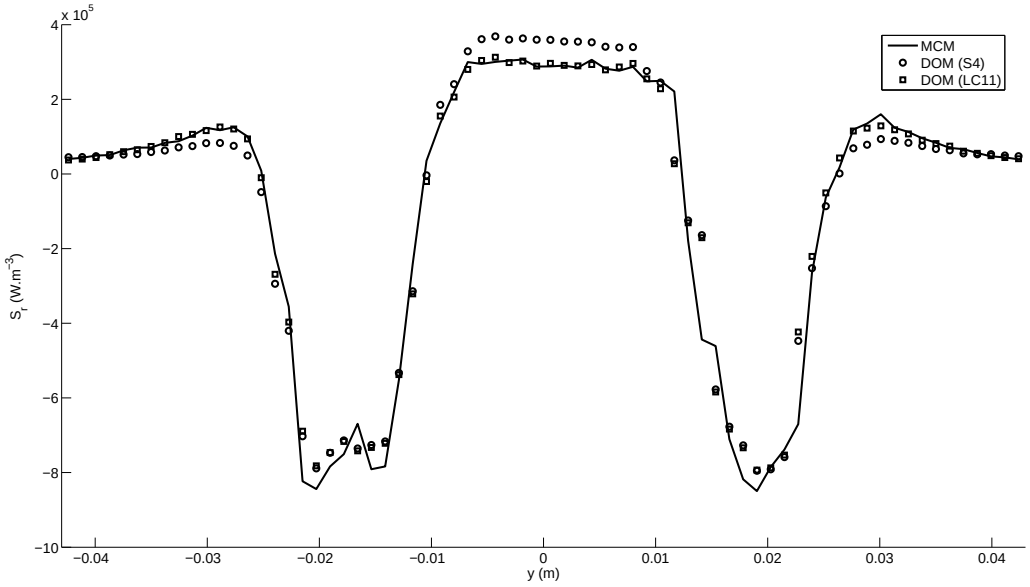

FIG. 10: Radiative source term along the y-axis axis located at $x = 0.02$m in the median plane of the combustion chamber. Calculation with DOM-S_4 quadrature, DOM-LC_{11} quadrature and MCM.

axis in Fig. 12 and 13). The averaged relative error on the MCM solution is found to be 3.17%.

The flame impact is well represented by the three methods. The solution modelled with the LC_{11} (96 discrete directions) is in excellent agreement with the reference solution, with a maximum error of 3%, confirming the already known high accuracy of this method. As expected the S_4 quadrature calculation is less accurate, in particular in the vicinity of the flame fronts. Note that the radiative source term is either underestimated (outside the conical flame) or overestimated (inside the conic flame), although the temperature and species concentrations are very close in these zones (Fig.12-13) and consequently the emission E is also very close in these zones (Fig.11).

We notice that the underestimation and the overestimation of the radiative source term S_r obtained with the S_4 quadrature are located in zones where temperatures and radiative species concentrations are the highest. This indicates that the error probably comes from a lack of angular resolution and illustrates clearly the benefit of the combined DOM-MCM approach : without the reference solution, it would be impossible to identify and estimate

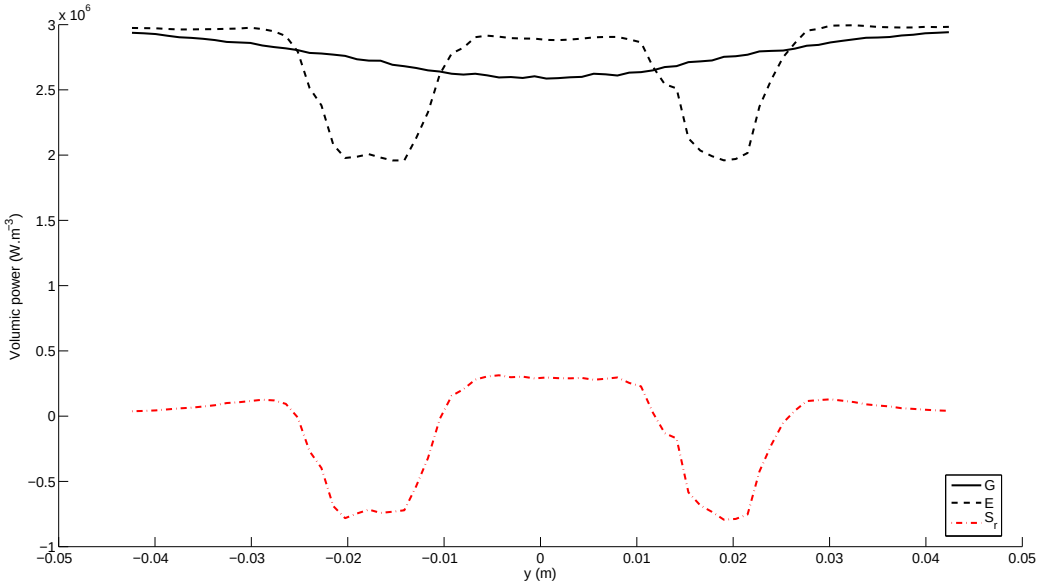

FIG. 11: Radiative incident heat flux G, radiative emitted heat flux E and radiative source term S_r along the y-axis axis located at $x = 0.02$m in the median plane of the combustion chamber. Calculation with DOM-LC_{11} quadrature.

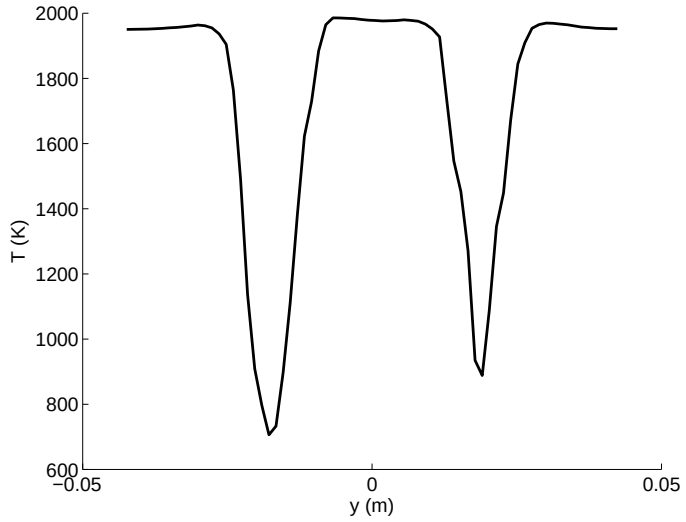

FIG. 12: Temperature profile along the y-axis axis located at $x = 0.02$m in the median plane of the combustion chamber.

such an error. Still the maximum error does not exceed 20% in very localized zones and one

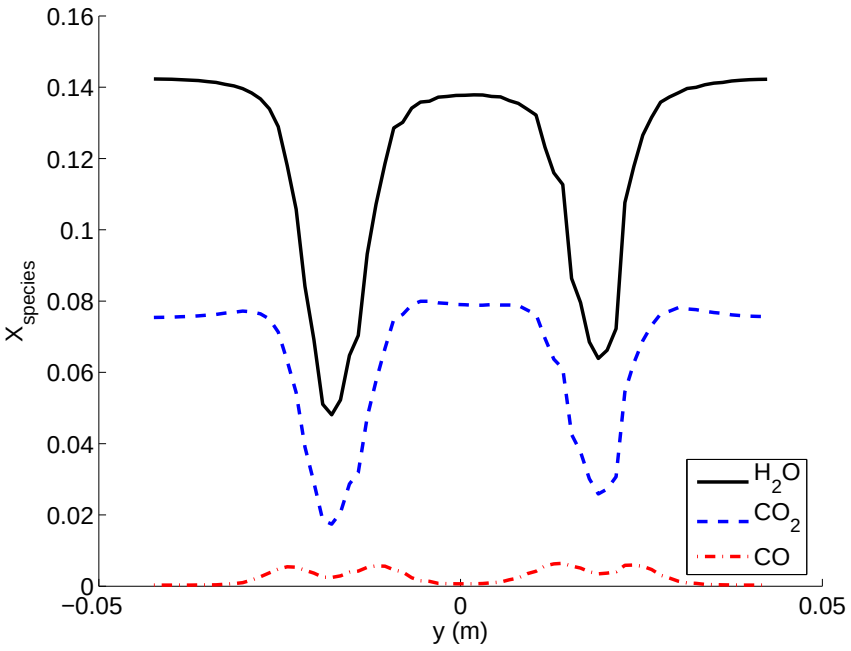

FIG. 13: Radiative species molar fractions profiles along the y-axis axis located at $x = 0.02$m in the median plane of the combustion chamber.

may conclude that for most combustion applications the accuracy of the DOM with the S_4 (24 discrete directions) quadrature is sufficient.

In the perspective of coupling radiation calculations with unsteady combustion simulations, the advantages of the combined DOM-MCM methodology appear also clearly in the light of CPU cost. While for the present case the DOM takes $4ms$/cell for each discrete direction, the MCM calculation time is of the order of a few seconds by point on the same computer.

CONCLUSIONS

The full coupling of radiation with unsteady combustion is a key point in the development of predictive simulation tools for industrial burners. It requires fast radiative models, with sufficient accuracy, as required by the combustion models. In this context, a combined DOM-MCM methodology is proposed, that cumulates the advantages of both classes of methods. The validity and potential of this methodology is demonstrated on both academic and complex industrial test cases. It is shown how the effective accuracy of an approximate

DOM solution is estimated with the MCM, allowing an optimal choice of parameters of the DOM and the best compromise between accuracy and rapidity.
The next step towards radiation-combustion coupled simulations is the improvement of computational ressources management and an automatic control procedure using simultaneously MCM. Simpler and faster spectral radiative properties models will also reduce the radiation computing time without significant loss of accuracy, down to a time of the same order of magnitude than the combustion simulations. These developments are currently in progress and first attempts of coupled simulations have already been successfull [33–36].

ACKNOWLEDGEMENT

The support of Turbomeca and the EC project PRECCINSTA (EU Contract ENK5-CT-2000-00060) is gratefully acknowledged for providing the CFD data.
Special thanks to Prof. Fournier of the University Paul Sabatier for his indications and fruitful discussions.

---

* E-mail:elhafi@enstimac.fr

[1] Beltrame A. et al Soot and NO formation in methane-oxygen enriched diffusion flames, Comb. and Flame 124, (2001), 295–310.

[2] Hall R.J., Smooke M.D. and Colket M.B., Predictions of soot dynamics in opposites jets diffusion flames, In Physical and chemical aspects of combustion, Glassman et al. Edition, (1997)

[3] Mbiock M. and Weber R., Radiation in enclosures, Springer-Verlag, 2000

[4] Jensen K.A., Ripoll J.F., Wray A. A., Joseph D., El Hafi M., On various modeling approaches for radiative heat transfer in pool fires, Combustion and Flame 148(4), (2007), 263–279.

[5] de Lataillade A., Dufresne J.L., El Hafi, M., Eymet V. & Fournier R., A net exchange Monte Carlo approach to radiation in optically thick systems, Jour. of Quant. Spectrosc. & Radiat.Transfer 74 (5), (2002), 563–584.

[6] Coelho P.J., Perez P., El Hafi M., Benchmark numerical solutions for radiative heat transfer in two-dimensional nongray sooting media, Numer. Heat Transfer B-Fund 43, (2003), 425–444.

[7] Perez P., El Hafi M., Coelho P.J. & Fournier R., Accurate solutions for radiative heat transfer in two-dimensional axisymetric enclosures with gas radiation and reflective surfaces., Numerical Heat Transfer, Part B , 46, (2005), 39–63.

[8] Tessé L., Dupoirieux F., Taine J., Monte Carlo Modeling of radiative transfer in a turbulent sooty flame, Int. J. Heat Mass Transfer 47, (2004), 555–572.

[9] Lataillade A., Blanco S., Clergent Y., Dufresne J.L., El Hafi M.,Fournier R., Monte Carlo Methods and sensitivity Estimations., Journal of Quantitative Spect. and Rad. Transfer 75, (2002), 529–538

[10] Roger M., Blanco S., El Hafi M., Fournier R., Monte Carlo Estimates of Domain Deformation Sensitivities, Phys. Review Letter 95, (2005), 180–601

[11] Modest, M.F., Radiative heat transfer. 3rd ed., McGraw-Hill, 2003.

[12] Liu J., Shang H.M., Chen Y.S., Wang T.S., Development of an unstructured radiation model applicable for two dimensional planar, axisymmetric and 3-dimensional geometries, J. Quant. Spectrosc. Radiat. Transfer 66, (2000), 17–33.

[13] Joseph D., El Hafi M., Fournier R., Cuenot B., Comparison of three spatial differencing schemes in Discrete Ordinates Method using three-dimensional unstructured meshes, Int. J. Thermal Sci. 44(9), (2005), 851–864.

[14] Lockwood, F. C., Shah, N.G., A new radiation solution method for incorporation in general combustion prediction procedures, Eighteenth Symposium (International) on Combustion, The Combustion Institute, (1981), 1405–1409.

[15] Joseph D., Modélisation des transferts radiatifs en combustion par méthode aux ordonnées discrètes sur des maillages non structurés tridimensionnels,Institut National Polytechnique de Toulouse (2004)

[16] Perez P., Algorithmes de synthèse d'images et propriétés spectrales des gaz de combustion : méthode de Monte Carlo pour la simulation des transferts radiatifs dans les procédés à haute température,Institut National Polytechnique de Toulouse (2003)

[17] Liu F., Numerical Solutions of Three-Dimensional Non-Grey Gas Radiative Transfer Using the Statistical Narrow-Band Model, Jour. Heat transfer 121, (1999), 200–203.

[18] Soufiani A., Taine J., High temperature gas radiative property parameters of statistical narrow band model for H_2O, CO_2 and CO and correlated-K model for H_2O and CO_2, Int. J. Heat Mass Transfer 40(4), (1997), 987–991.

[19] Chandrashekhar S., Radiative transfer, Clarendon Press, Oxford, 1950.

[20] Koch R., Becker R., Evaluation of the Quadrature Schemes for the Discrete Ordinates Method, in: Lybaert P., Feldheim V., Lemonnier D., Selçuk N. (Eds), Proceedings of Eurotherm73 on Computational Thermal Radiation in Participating Media, Eurotherm Series 11, Elsevier, Paris, France, (2003), 59–74.

[21] Ströhle J., Schnell U., Hein K.R.G., A Mean Flux Discrete Ordinates Interpolation scheme for general coordinates, 3rd International Conference on Heat Transfer, Antalya, (2001).

[22] Liu F., Smallwood G.J., Gülder Ö.L., Application of the statistical narrow-band correlated-k method to low-resolution spectral intensity and radiative heat transfer calculations - Effects of the quadrature scheme, Int. J. Heat Mass Transfer 43, (2000), 3119–3135.

[23] Liu F., Smallwood G.J., Gülder Ö.L., Application of the statistical narrow-band correlated-k method to non-grey gas radiation in CO_2-H_2O mixtures: approximate treatments of overlapping bands, J. Quant. Spectrosc. Radiat. Transfer 68, (2001), 401–417.

[24] Hottel, H.C. and Sarofim, A.F., Radiative transfer, McGraw-Hill Book Company, 1967.

[25] Green, J.S.A., Division of radiative streams into internal transfer and cooling to space, Quaterly Journal of the Royal Meteorological Society 93, (1967), 371–372.

[26] Cherkaoui, M., Dufresne, J.L., Fournier, R., Grandpeix, J.Y. & Lahellec, A., Monte Carlo simulation of radiation in gases with a narrow-band model and a net-exchange formulation, Jour. of Heat Transfer 118, (1996), 401–407.

[27] Dufresne J-L., Fournier R., Grandpeix J-Y., Inverse Gaussian K-distributions, J. Quant. Spectrosc. Radiat. Transfer 61, (1999), 433–441.

[28] Schönfeld T., Rudgyard. M., Steady and unsteady flows simulations using the hybrid flow solver AVBP AIAA Journal 37(11), (1999), 1378–1385

[29] Roux S., Lartigue G., Poinsot T., Meier U., Bérat. C., Studies of mean and unsteady flow in a swirled combustor using experiments, acoustic analysis and large eddy simulations, Combustion and Flame 141, (2005), 40–54.

[30] Angelberger, C., Egolfopoulos, F. and Veynante, D., Large eddy simulations of chemical and acoustic forcing of a premixed dump combustor, Flow Turb. and Combustion 65(2), (2000), 205–222.

[31] Colin, O., Ducros F., Veynante D. and Poinsot, T.,A thickened flame model for large eddy simulations of turbulent premixed combustion,Phys. Fluids 12(7), (2000), 1843–1863.

[32] Selle, L., Lartigue, G., Poinsot, T., Koch, R., Schildmacher, K.U., Krebs, W., Prade, B., Kaufmann, P. and Veynante, D., Compressible large eddy simulations of turbulent combustion on complex geometries on unstructured meshes, Combustion and Flame 137, (2004), 489-505.

[33] R. Goncalves dos Santos, M. Lecanu, S. Ducruix, O. Gicquel and D. Veynante, Large eddy simulations of combustion / radiative heat transfers coupling using the specialized communication language CORBA, The Cyprus International Symposium on Complex Effects in Large Eddy Simulations, Limassol, Cyprus, September 20-25, (2005).

[34] R. Gonçalves dos Santos, S. Ducruix, O. Gicquel, and D. Veynante, Large Eddy Simulations of Turbulent Combustion Including Radiative Heat Transfers using Specialised Communication Languages, 11th International Conference on Numerical Combustion, Granada, Spain (2006).

[35] R. Gonçalves dos Santos, S. Ducruix, O. Gicquel, D. Joseph, M. El Hafi and D. Veynante, Large-eddy simulations including radiative heat transfer, 3rd European Combustion Meeting, paper 23-3, Chania, Crete, April 11-13, (2007).

[36] R. Goncalves dos Santos, M. Lecanu, S. Ducruix, O. Gicquel, E. Iacona and D. Veynante, Coupled large eddy simulations of turbulent combustion and radiative heat transfer, Combustion and Flame 152(3), 387-400.

List of Captions for the Figures

Fig. 1 Radiative source terme along the central axis of the cylinder.

Fig. 2 Relative error associated to the MCM radiative source term along the central axis of the cylinder.

Fig. 3 Incident radiative heat flux at the wall of the cylinder.

Fig. 4 Relative error associated to the MCM incident radiative heat flux at the wall of the cylinder.

Fig. 5 Cylindrical grid (100,000 cells).

Fig. 6 Grid of the combustion chamber.

Fig. 8 Instantaneous solution fields in the median cutting plane of the combustion chamber: temperature and radiative species concentration.

Fig. 8(a) Temperature profile

Fig. 8(b) X_{H_2O} profile

Fig. 8(c) X_{CO_2} profile

Fig. 8(d) X_{CO} profile

Fig. 7 Instantaneous heat release $\dot{\omega}$ in the median cutting plane of the combustion chamber.

Fig. 9 Instantaneous radiative source term in the median cutting plane of the combustion chamber. Calculation with DOM-S_4 quadrature.

Fig. 10 Radiative source term along the y-axis axis located at $x = 0.02$m in the median plane of the combustion chamber. Calculation with DOM-S_4 quadrature, DOM-LC_{11} quadrature and MCM.

Fig. 12 Temperature profile along the y-axis axis located at $x = 0.02$m in the median plane of the combustion chamber.

Fig. 13 Radiative species molar fractions profiles along the y-axis axis located at $x = 0.02$m in the median plane of the combustion chamber.

Fig. 11 Radiative incident heat flux G, radiative emitted heat flux E and radiative source term S_r along the y-axis axis located at $x = 0.02$m in the median plane of the combustion chamber. Calculation with DOM-LC_{11} quadrature.